Correspondence

Range Sidelobe Level Reduction With a Train of Diverse LFM Pulses

Target masking is a pervasive problem in radar signal processing: the range sidelobes of the waveform's matched filter response may cause a strong target to prevent the detection of nearby weaker targets. Common solutions to sidelobe level reduction for frequency-modulated waveforms result in a signal-to-noise ratio (SNR) loss. In this correspondence, we propose a novel method using pulse diversity to reduce the range sidelobes while avoiding an SNR loss. The proposed approach is based on shaping the power spectrum of the summation of a train of constant-amplitude linearly frequency-modulated pulses to resemble a Gaussian function. We present a numerical example demonstrating a drastic sidelobe level reduction. Importantly, our approach avoids any processing SNR loss.

I. INTRODUCTION

In the state-of-the-art radar systems, frequency-modulated (FM) waveforms are commonly used to simultaneously achieve a high signal-to-noise ratio (SNR) and good range resolution [1]. Linear frequency modulation (LFM) is the most common FM waveform due to its ease of generation and Doppler tolerance. Pulse compression using the matched filter (MF) is the optimum SNR strategy for processing the received signal. However, for a waveform with a uniform spectrum, the MF output has undesirable high-range sidelobes close to the mainlobe response. The sidelobes of a strong SNR target may mask a nearby weak SNR target, preventing its detection. Moreover, the sidelobes of a strong target may be mistakenly declared as separate targets themselves.

Several methods for reducing the sidelobe level (SLL) of the waveform's pulse-compressed response exist in the literature. Most of the proposed methods deal with designing discrete phase-modulated (PM) sequences with desirable correlation properties (e.g., [2]–[6]). For FM (i.e., continuously PM) pulses, a simple way to reduce the SLL is to apply a linear amplitude weighting function to the time domain signal [1]. The mismatched filters (e.g., inverse filter) [7]–[9] and the nonlinear FM (NLFM) waveform [1] can also be designed to reduce the SLL. Another method is to use so-called complementary codes, which have been demonstrated for FM [10] and PM waveforms [11]. In

Manuscript received March 9, 2021; revised June 22, 2021; released for publication September 22, 2021. Date of publication September 30, 2021; date of current version April 12, 2022.

DOI. No. 10.1109/TAES.2021.3115991

Refereeing of this contribution was handled by S. Blunt.

Authors' addresses: Nadav Neuberger is with the Fraunhofer Institute for High Frequency Physics and Radar Techniques FHR, 53343 Wachtberg, Germany; E-mail: (nadav.neuberger@fhr.fraunhofer.de); Risto Vehmas is with Elettronica GmbH, 53340 Meckenheim, Germany, E-mail: (r.vehmas@elettronica.de). *(Corresponding author: Nadav Neuberger.)*

our previous work, we proposed a Costas-based frequency coding to design a low SLL area in the range-Doppler domain [12].

The abovementioned approaches have their associated drawbacks: the SNR or the range resolution may be degraded, the processing and hardware complexity is often increased, and the sidelobe suppression may be sensitive to a Doppler shift. In applications requiring sensitive target detection at very large ranges, a loss in SNR is undesirable. The purpose of this correspondence is to present a novel concept for SLL reduction without any SNR loss.

Due to the improvements in radar hardware and processing power, there has been significant interest in pulse diverse waveforms [13]. The term pulse diversity refers to changing the modulation parameters and applying a different processing filter from pulse to pulse. Previously, pulse diversity has received attention in SLL reduction for PM waveforms [14]. Additionally, diverse random FM [15] and LFM [16] waveforms have been proposed as well. These references describe various advantages of using diverse pulse trains, but do not deal with reducing the SLL in a systematic way.

In this correspondence, we propose novel methods to reduce the SLL of an LFM waveform using a train of diverse pulses. The diversity of the pulse train is achieved by allowing the duration or the bandwidth of each pulse to change. Conceptually, our methods are similar to the chirp diverse waveform [16], which is based on using a train of LFM pulses with a different chirp rate. As an important novelty, our methods are based on optimizing the power spectrum of the diverse LFM pulse train. By shaping the spectrum to resemble a Gaussian function, we achieve a significant SLL reduction for the waveform's autocorrelation function (ACF). Significantly, our methods avoid the SNR loss caused by the receive filter, which is unavoidable when using mismatched filters. The drawbacks of our approach are wider ACF mainlobe width (degraded range resolution) and an increased complexity for signal generation and processing.

II. WAVEFORM DESIGN METHOD

A. Motivation

According to the well-known Wiener–Khinchin theorem [17], the inverse Fourier transform (FT) of the power spectrum of a signal is the ACF of the signal. Thus, it is possible to obtain desirable properties for the waveform's ACF by tuning its power spectrum. For example, the inverse FT of a Gaussian power spectrum produces a Gaussian ACF without sidelobes. To achieve a nearly Gaussian spectrum for the waveform, a common method is to use linear amplitude weighting in the time domain. This can be done for both the transmitted and received signals or only for the received signal. In the latter case, this means that the MF is replaced by a mismatched filter, which acts as a spectral window to reduce the SLL. However, both options have their drawbacks, the most important being a loss in SNR [1].

By allowing the duration and bandwidth of each FM pulse to change, we can manipulate the power spectrum of the waveform. For example, by appropriately choosing the bandwidth of each pulse, a nearly Gaussian shape can be achieved. Thus, we can reduce the SLL without amplitude weighting or resorting to mismatched filters (avoiding SNR loss). Compared to a train of identical pulses with a uniform spectrum, the main drawback is a degraded range resolution.

B. Signal Model

We consider a monostatic radar system transmitting a train of diverse LFM pulses. We assume that the maximum available bandwidth B and pulse duration T are given. The baseband LFM train of M pulses can be expressed as

$$x(t) = \sum_{m=1}^{M} p_m(t) \tag{1}$$

where the mth pulse is defined as

$$p_m(t) = \text{rect}\left(\frac{t - mT_{\text{PRI}}}{T_m}\right) \exp\left(-i\pi\gamma_m(t - mT_{\text{PRI}})^2\right) \tag{2}$$

and T_{PRI} is the pulse repetition interval (PRI), T_m is the pulse duration, $\gamma_m = B_m/T_m$ is the chirp rate, and B_m is the bandwidth of the mth pulse. We assume that the receiver bandwidth is kept constant for each pulse despite the changing signal bandwidth. This way the noise power spectral density (PSD) is constant for each pulse. If the receiver bandwidth changes from pulse to pulse, the amplitude of each pulse can be scaled to retain a constant noise PSD.

We consider two possible ways to use LFM pulse diversity.

1) Changing both the bandwidth $B_m = a_m B$ and the duration $T_m = a_m T$ of the mth pulse by the same factor a_m.
2) Changing only the bandwidth $B_m = a_m B$ and keeping the duration $T_m = T$ fixed.

The weights $0 < a_m \leq 1$ are chosen to achieve a nearly Gaussian power spectrum for the pulse train. In both options, we set $a_M = 1$ for the last pulse (i. e. $T_M = T$ and $B_M = B$). The optimization procedure to achieve this is described in the next section. One the one hand, for option 1), the chirp rate $\gamma_m = B_m/T_m = B/T$ is constant for all pulses in the train. On the other hand, for the second option, $\gamma_m = B_m/T_m = a_m B/T$ changes from pulse to pulse.

Assuming that the received signal is corrupted by white Gaussian noise, the MF response of the waveform can be expressed using the ACF as

$$\text{ACF}(\tau) = \int_{-\infty}^{\infty} x(t)x^*(t+\tau)dt \tag{3}$$

where τ is the time delay variable. When using a mismatched filter, the pulse-compressed signal is represented by the cross-correlation between x and the mismatched filter. In the following sections, we will carefully analyze the ACF to study the performance of the proposed pulse trains.

C. Limitations

While pulse train 1) results in an SNR loss due to shorter transmit (Tx) duration (assuming limited maximum Tx power), the second option suffers no loss of energy. We note that if the radar hardware permits the Tx power to be increased when using a lower duty cycle, the SNR loss may be avoided for option 1) as well.

In general, the performance of the proposed methods is sensitive to both a Doppler shift between the pulses and range walk, when these are not properly compensated (e.g., by using keystone or backprojection transformations). Another limitation of our methods concerns a lower slow-time sampling rate of the highest frequencies $|f| \approx B/2$. Since these frequencies appear only in one of the pulses in the train, they are sampled at a rate of PRF/M (where PRF is the pulse repetition frequency), i.e., only once every coherent processing interval (CPI). For fast moving targets with a high Doppler frequency, this may lead to aliasing of the Doppler spectrum.

In many systems, the amount of raw data is reduced by presumming prior to pulse compression, reducing the data rate. A possible drawback of the proposed methods is that presumming cannot be used, resulting in a higher data rate and volume.

D. Power Spectrum Optimization

We aim to shape the power spectrum of the LFM train to be a Gaussian by tuning the waveform parameters appropriately. Since a Gaussian spectrum theoretically produces a Gaussian ACF, we can minimize both the total sidelobe energy [integrated sidelobe ratio (ISLR)] and maximum sidelobe value [peak-to-sidelobe ratio (PSLR)] simultaneously by optimizing the power spectrum.

We note that it is also possible to reduce the SLL by minimizing the ACF energy outside the mainlobe. However, this does not necessarily guarantee that both the ISLR and PSLR are minimized simultaneously. This issue could be resolved by minimizing a function of both ISLR and PSLR using constrained optimization. In this correspondence, we only focus on the spectrum optimization.

To avoid any processing losses, we only change the duration T_m and bandwidth B_m of each LFM pulse in the train. As an input, our method requires the maximum duration T and maximum bandwidth B allowed for a single pulse in the train. The last input is the shape parameter σ of the desired Gaussian power spectrum

$$G(f) = \exp\left(-\sigma f^2\right). \tag{4}$$

In choosing σ, it should be noted that the number of pulses M determines the maximum attenuation—$1/M$ in case of pulse train 1)—of the power spectrum at the edges ($f = \pm B/2$). Thus, it is useful to define σ in terms of the attenuation level $G_0 = G(B/2) = G(-B/2)$ at the edge of the spectrum. This results in

$$\sigma = -\frac{4\log G_0}{B^2}. \tag{5}$$

To obtain a Gaussian spectrum for the LFM train, we minimize the mean square error loss function

$$L(\boldsymbol{a}) = \int_{-\frac{B}{2}}^{\frac{B}{2}} |G(f) - X(f;\boldsymbol{a})|^2\, df \tag{6}$$

where

$$X(f;\boldsymbol{a}) = \int_{-\infty}^{\infty} \mathrm{ACF}(\tau;\boldsymbol{a}) e^{-i2\pi f\tau}\, d\tau \tag{7}$$

is the power spectrum of the LFM pulse train. The weights a_m are the variables we aim to optimize. They control the chirp rates γ_m and durations T_m of the pulses x_m. Thus, the waveform x, ACF, and power spectrum X in (7) depend on the weight vector $\boldsymbol{a} = [a_1 \ \ldots \ a_{M-1}]^T$.

We resort to numerical optimization to solve the minimization problem $\arg\min\{L(\boldsymbol{a})\}$. The reason for choosing this approach is twofold. First, there is no closed form solution for the optimal values a_m (minimizing L). Second, while a simple approximate solution to the problem can be found by using linearly increasing a_m or by quantizing the Gaussian with uniform steps, the accuracy of these methods degrades when M increases. Nevertheless, these simple solutions can be used to initialize the optimization.

III. NUMERICAL RESULTS

In this section, we demonstrate an application of the proposed diverse LFM trains in an important emerging radar application: space surveillance of targets in the low Earth orbit (LEO) region. In this context, a so-called fragmentation event where a large object (e.g., a satellite or large space debris particle) breaks down into multiple smaller debris particles, is of special interest. These debris particles, which originate from the same object, usually maintain the same orbital velocity in a close proximity from one another and pose a serious threat to active satellites [18], [19]. Thus, it is important to detect such events and accurately identify closely spaced targets of largely varying size (and thus SNR). Hence, the SLL has a major impact on this ability (together with the range resolution).

A. Simulation Setup

We consider the GESTRA system [20], which has the parameters $B = 2$ MHz and $T = 8.5$ ms. The number of coherently processed pulses M for GESTRA varies between 8 and 24, depending on the specific operation mode. For the following numerical demonstration, we consider $5 \le M \le 25$.

We simulated and compared the pulse-compressed responses of four different LFM pulse trains. In all cases, the PRI, available bandwidth B, and maximum pulse duration T are identical. In this example, the LFM pulses were implemented in a discrete manner—i.e., as a sum of constant frequency subpulses called chips with a continuous phase between the chips. For the mth pulse

$$N_m^c = \lfloor\sqrt{B_m T_m}\rfloor, \ T_m^c = T_m/N_m^c \ \text{ and } \ \Delta f_m = 1/T_m^c \tag{8}$$

where N_m^c is the number of chips, T_m^c the chip duration, and Δf_m the frequency step [1]. The chip implementation is used to provide a realistic simulation for the GESTRA system. Our method can just as easily be used for a continuous LFM implementation. With the parameters described previously, the chip-wise implementation very closely approximates a continuous LFM.

We compare the proposed pulse trains with two benchmark pulse trains. The first train denoted as x_0 is composed of identical LFM pulses, each of bandwidth B and duration T ($a_m = 1$ for $m = 1, \ldots, M$). This pulse train serves as the first benchmark for the SLL reduction performance. The train denoted as x_3 is the same as x_0, where a mismatched filter [with the frequency response G from (4)] is used for pulse compression. Ideally, this method perfectly shapes the spectrum, and thus provides a second benchmark for assessing our method. The trains denoted by x_1 and x_2 correspond to options 1) and 2) in Section II-B, respectively.

In the following simulations, the target spectrum shape G for x_1 and x_2 is an ideal Gaussian such that the power is attenuated to $1/M$ at the edge of the full available bandwidth B, i.e., $G_0 = 1/M$ and $\sigma = 4 \log M/B^2$. The reason for this choice is clarified in Section III-D.

To obtain a solution to $\arg\min\{L(\boldsymbol{a})\}$, we chose the simultaneous perturbation stochastic approximation method [21], due to its computational efficiency and ease of implementation. For simplicity, $\boldsymbol{a}_1$ and $\boldsymbol{a}_2$ are chosen to be monotonically increasing. We note that other arrangements of the same values will have identical results for the ACF—i.e., the zero-Doppler cut of the ambiguity function. However, the performance may differ in case there is a Doppler shift due to target motion.

B. Performance Metrics

To evaluate the SLL reduction performance for the ACF, we use three figures of merit: 1) range resolution $\Delta R = c\Delta\tau_{3\,\mathrm{dB}}/2$, where $\Delta\tau_{3\,\mathrm{dB}}$ is the 3 dB width of the mainlobe of $|\mathrm{ACF}|^2$ in time units, and c is the speed of light; 2) PSLR; and 3) ISLR.

The ISLR is defined as

$$\begin{aligned} \mathrm{ISLR} &= \frac{\sum_\Theta |\mathrm{ACF}(\tau)|^2}{\sum_\Delta |\mathrm{ACF}(\tau)|^2} \\ \Theta &:= \{-T \le \tau < -\Delta\tau_0\} \cup \{\Delta\tau_0 < \tau \le T\} \\ \Delta &:= \{-\Delta\tau_0 \le \tau \le \Delta\tau_0\} \end{aligned} \tag{9}$$

where Θ represents the sidelobe delays, Δ corresponds to the delays within the mainlobe, and $\Delta\tau_0$ is the null-to-null beamwidth of the mainlobe. The PSLR is defined as

$$\mathrm{PSLR} = \left|\frac{\mathrm{ACF}(0)}{\rho_{\mathrm{SL}}}\right|^2, \text{ where } \rho_{\mathrm{SL}} = \max_{\tau\in\Theta} |\mathrm{ACF}(\tau)|. \tag{10}$$

The PSLR quantifies both the false detections due to high sidelobes as well as the worst-case scenario for masking of closely spaced targets. On the other hand, the ISLR quantifies the average masking, as it takes into account the total sidelobe energy over the time delay (range) domain.

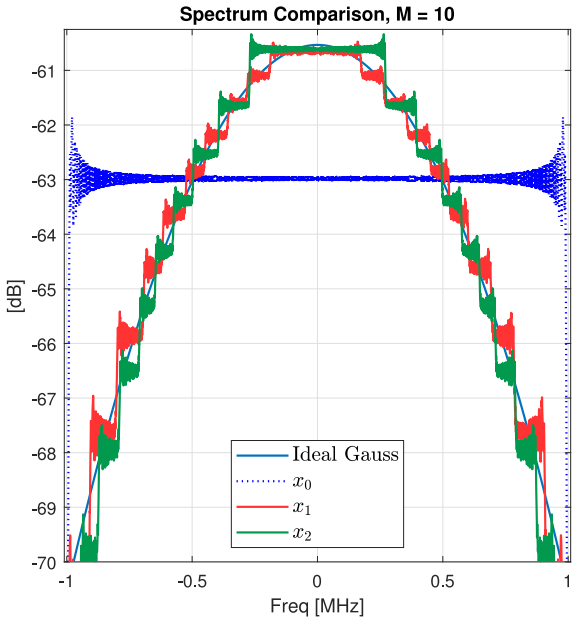

Fig. 1. Normalized power spectrums of the various LFM trains alongside the ideal Gaussian function.

Another important consideration is the waveform's sensitivity to a Doppler mismatch. Since the SLL suppression is achieved by coherently combining the pulses, an uncompensated phase difference (due to the target's movement) between the pulses may hinder the SLL suppression.

The worst-case scenario for the Doppler mismatch is determined by the spacing in the Doppler filter bank that is used to coherently process the pulses. We assume this spacing to be determined by the theoretical Doppler resolution $\Delta f_d = 1/[(M-1)T_{\mathrm{PRI}} + T_M]$, which is the inverse of the coherent processing time. This mismatch results in a phase difference of $\Delta\phi = \pi\Delta f_d T_{\mathrm{PRI}}$ between two adjacent pulses. In the simulations, this effect is taken into account by multiplying each received pulse p_m with a phase term $\exp(i\pi\Delta f_d(m-1)T_{\mathrm{PRI}})$, where m is the pulse number.

Finally, we note that for the GESTRA parameters, the range walk for a LEO target can be very accurately compensated using keystone formatting or back-projection [22]. As an example, the worst-case Doppler mismatch Δf_d corresponds to a residual range walk of about 1 m during a CPI of $M = 24$ pulses, which is negligible when compared with the range resolution $\Delta R \approx 75$ m. For this reason, the range walk is omitted from the simulations.

C. Performance Comparison

We begin this section by choosing a single case of $M = 10$ to illustrate the various aspects of the proposed methods. Fig. 1 shows the power spectrums of the different pulse trains. The step-wise spectrum structure of x_1 and x_2 is evident. The attenuation at the edges matches the desired $1/M$, with an overall good fit. In Fig. 2, a zoom in of the vicinity of the mainlobe in $|\mathrm{ACF}|^2$ is presented. The lower SLLs of x_1 and x_2 ($\approx$18 dB lower than for x_0) are clearly seen, along with a widening of the mainlobe. A broader view

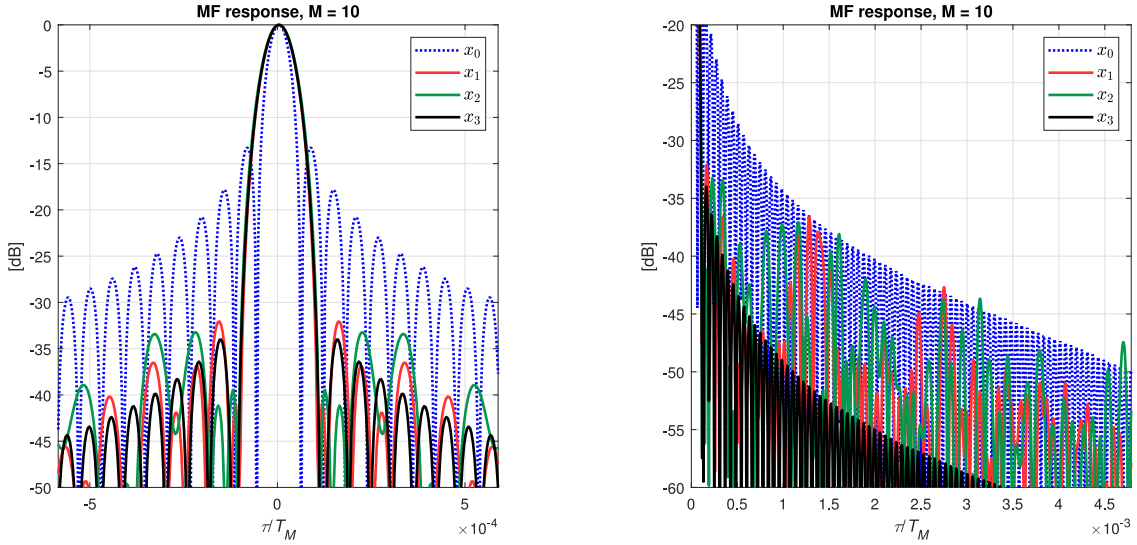

Fig. 2. ACF power for each of the simulated pulse trains. The mainlobe and first sidelobes are shown on the left, whereas the plot on the right shows the sidelobes farther away. A notable SLL suppression is achieved with a penalty in range resolution. The proposed pulse trains x_1 and x_2 nearly achieve the SLL suppression of the spectral windowing method x_3.

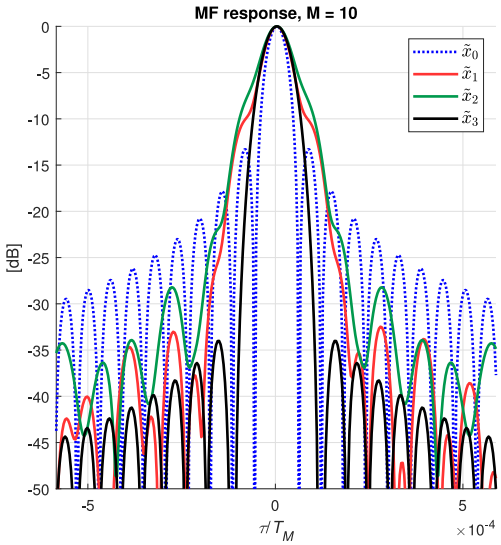

Fig. 3. MF power responses in the presence of a Doppler mismatch. For the proposed pulse trains, the worst-case mismatch results in a degraded range resolution and increased SLLs.

is also given, where longer delay sidelobe peaks emerge (with very high attenuation, rendering them insignificant).

To investigate the effect of a Doppler mismatch, we simulated an uncompensated phase difference $\Delta\phi$ between the pulses in each of the trains. Then, for calculating the MF response, the train x_i without the Doppler shift was used as the MF. The pulse-compressed MF outputs are depicted in Fig. 3, where these cases are denoted by $\tilde{x}_i$, the subscripts remaining the same as above. We see that $\tilde{x}_1$ presents the highest Doppler mismatch sensitivity, with 5 dB PSLR and 3 dB ISLR degradation. In general, the worst-case Doppler mismatch degrades the SLL suppression for the proposed trains, though not very significantly. Moreover, the width of the mainlobe is slightly increased. We note that these effects can be mitigated by using a finer Doppler grid, leading to a smaller Δf_d. However, this would lead to increasing the computational load of the processing.

The SNR loss computation for each one of the trains is a crucial aspect in many applications. Assuming that the Tx power per time unit is constantly at maximum level, which is a common practical constraint, x_1 has a lower Tx power compared to x_0 (due to shorter pulses). This results in an SNR loss—not due to processing, but to a limited maximum Tx power. This loss can be quantified by $(MT_M)^{-1}\sum_{m=1}^{M} T_m$. In the case where the spectrum of x_1 in Fig. 1 is achieved using the linear amplitude weighting method (i.e., by weighting each pulse of x_0 with a linear amplitude taper), there will be an SNR loss of 2.4 dB. The mismatched filtering (spectral windowing) method x_3 results in a mismatch loss, which depends on the spectral window G. More specifically, for a Gaussian window, the SNR loss increases with increasing value of σ (see [1] for detailed calculations). In contrast, there is no SNR loss to x_2 due to the fixed pulse duration.

We investigated the effect of increasing M in the above-mentioned performance metrics as well as the SNR loss. The results of these simulations are shown in Fig. 4. As an example, when choosing x_2 and exploiting the full number of available pulses in GESTRA, it is possible to improve the PSLR level by up to 31 dB and the ISLR by up to 20 dB (compared to x_0), while the range resolution is degraded by 60%. Importantly, this is achieved without any SNR loss.

As expected, the mismatched filtering x_3 achieves the best SLL suppression. However, the proposed pulse trains x_1 and x_2 also perform very well: there is only a difference of a few decibels in PSLR. In the ISLR, the difference is more pronounced (up to 5 dB). This can also been seen from the ACF plots in Fig. 2. The ripples in the power spectra of x_1 and x_2 result in higher sidelobes for large delays when compared with x_3. The range resolution remains similar to a large degree of accuracy for each of the trains x_1, x_2, and

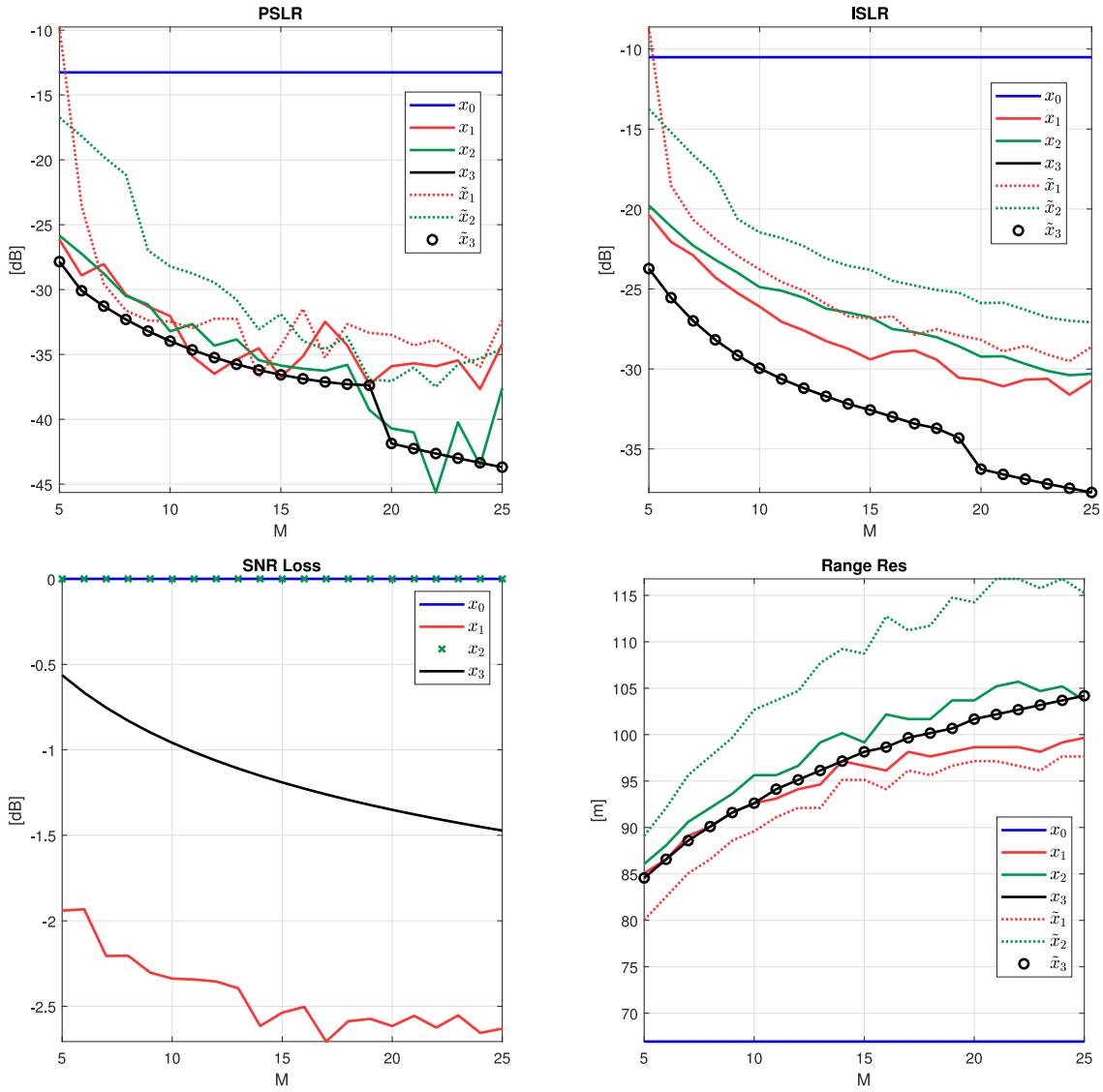

Fig. 4. Performance metrics of the different pulse trains. While the mismatched filtering (x_3) provides the best SLL performance, it results in a loss of SNR increasing with the number of pulses M.

x_3. Importantly, we prove that the SLL suppression for x_2 is achieved without any SNR loss for all cases, while it increases with M for x_3.

D. Discussion

In our experiments, we always set $\sigma = 4 \log M/B^2$ so that the attenuation at the edge of the spectrum $G_0 = 1/M$. We found this to be a reasonable strategy since using a higher σ (lower G_0) would make it impossible to achieve a good fit near the edges of the spectrum. Moreover, we observed that when using a fixed value for σ, increasing M did not result in a better result. This is demonstrated in Fig. 5 for the attenuation level of $G_0 = 1/10$. When the number of pulses increases beyond $M = 10$ (keeping G_0 and thus σ fixed), it becomes challenging to prevent a higher attenuation at the edges while simultaneously obtaining a good fit with the ideal Gaussian G.

We conclude that x_2 is the most beneficial choice in our example—taking into account the SLL reduction, range resolution, and SNR loss together. It should be noted that even though the results of x_1 could, in theory, be closely achieved by the amplitude weighting method, our approach is easier to implement from a hardware perspective (Tx power level is constant). In case the radar hardware permits increasing the Tx power when the duty cycle is lowered, the SNR loss of x_1 can possibly be mitigated.

IV. CONCLUSION

In this correspondence, we presented methods to lower the range sidelobes by using a diverse train of LFM pulses. Notably, our approach suffers no processing loss in SNR, the improvement comes only at the cost of degraded range resolution and increased processing complexity. A significant reduction in both the PSLR and ISLR closely approaching the performance of the common mismatched filtering method was demonstrated in a simulated example related to a practical application of the waveform.

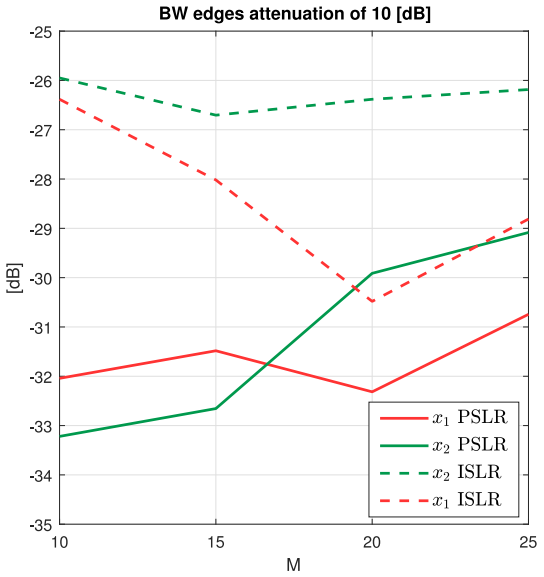

Fig. 5. SLL performance metrics for the proposed pulse trains as a function of the number of pulses M for a fixed Gaussian shape.

Future work entails investigating the effect of the number of pulses on the performance, as well as the Gaussian optimization method with different parameters and additional FM waveforms.

NADAV NEUBERGER
Fraunhofer Institute for High Frequency Physics and Radar Techniques FHR
Wachtberg, Germany

RISTO VEHMAS
Elettronica GmbH Meckenheim, Germany

REFERENCES

[1] N. Levanon and E. Mozeson
Radar Signals. Hoboken, NJ, USA: Wiley, 2004.

[2] P. Stoica, H. He, and J. Li
New algorithms for designing unimodular sequences with good correlation properties
IEEE Trans. Signal Process., vol. 57, no. 4, pp. 1415–1425, Apr. 2009.

[3] P. Stoica, H. He, and J. Li
On designing sequences with impulse-like periodic correlation
IEEE Signal Process. Lett., vol. 16, no. 8, pp. 703–706, Aug. 2009.

[4] M. Soltanalian and P. Stoica
Computational design of sequences with good correlation properties
IEEE Trans. Signal Process., vol. 60, no. 5, pp. 2180–2193, May 2012.

[5] J. Song, P. Babu, and D. P. Palomar
Optimization methods for designing sequences with low autocorrelation sidelobes
IEEE Trans. Signal Process., vol. 63, no. 15, pp. 3998–4009, Aug. 2015.

[6] J. Song, P. Babu, and D. P. Palomar
Sequence design to minimize the weighted integrated and peak sidelobe levels
IEEE Trans. Signal Process., vol. 64, no. 8, pp. 2051–2064, Apr. 2016.

[7] M. H. Ackroyd and F. Ghani
Optimum mismatched filters for sidelobe suppression
IEEE Trans. Aerosp. Electron. Syst., vol. AES-9, no. 2, pp. 214–218, Mar. 1973.

[8] S. D. Blunt, M. Cook, J. Jakabosky, J. de Graaf, and E. Perrins
Polyphase-coded FM (PCFM) radar waveforms, part I: Implementation
IEEE Trans. Aerosp. Electron. Syst., vol. 50, no. 3, pp. 2218–2229, Jul. 2014.

[9] D. Henke, P. McCormick, S. D. Blunt, and T. Higgins
Practical aspects of optimal mismatch filtering and adaptive pulse compression for FM waveforms
In *Proc. IEEE Radar Conf.*, 2015, pp. 1149–1155.

[10] C. C. Jones, C. A. Mohr, P. M. McCormick, and S. D. Blunt
Complementary frequency modulated radar waveforms and optimised receive processing
IET Radar Sonar Navigation, vol. 15, pp. 708–723, Apr. 2021.

[11] M. Li, K. S. Ho, and G. Hayward
Beamspace transformation for data reduction using genetic algorithms
In *Proc. IEEE Int. Ultrasonics Symp.*, 2009, pp. 702–705.

[12] N. Neuberger and R. Vehmas
A Costas-based waveform for local range-Doppler sidelobe level reduction
IEEE Signal Process. Lett., vol. 28, pp. 673–677, Mar. 2021.

[13] S. D. Blunt and E. L. Mokole
Overview of radar waveform diversity
IEEE Aerosp. Electron. Syst. Mag., vol. 31, no. 11, pp. 2–42, Nov. 2016.

[14] N. Levanon, I. Cohen, and P. Itkin
Complementary pair radar waveforms-evaluating and mitigating some drawbacks
IEEE Aerosp. Electron. Syst. Mag., vol. 32, no. 3, pp. 40–50, Mar. 2017.

[15] S. D. Blunt *et al.*
Principles and applications of random FM radar waveform design
IEEE Aerosp. Electron. Syst. Mag., vol. 35, no. 10, pp. 20–28, Oct. 2020.

[16] V. C. Vannicola, T. B. Hale, M. C. Wicks, and P. Antonik
Ambiguity function analysis for the chirp diverse waveform (CDW)
In *Rec. IEEE Int. Radar Conf. [Cat. No. 00CH37037]*, 2000, pp. 666–671.

[17] N. Wiener
Generalized harmonic analysis
Acta Mathematica, vol. 55, pp. 117–258, 1930.

[18] A. Murtaza, S. J. H. Pirzada, T. Xu, and L. Jianwei
Orbital debris threat for space sustainability and way forward
IEEE Access, vol. 8, pp. 61000–61019, Mar. 2020.

[19] D. Vallado and D. Oltrogge
Fragmentation event debris field evolution using 3D volumetric risk assessment
In *Proc. 7th Eur. Conf. Space Debris*, 2017, pp. 1–18.

[20] H. Wilden *et al.*
GESTRA – A phased-array based surveillance and tracking radar for space situational awareness
In *Proc. IEEE Int. Symp. Phased Array Syst. Technol.*, 2016, pp. 1–5.

[21] J. C. Spall
Implementation of the simultaneous perturbation algorithm for stochastic optimization
IEEE Trans. Aerosp. Electron. Syst., vol. 34, no. 3, pp. 817–823, Jul. 1998.

[22] H. Wilden *et al.*
GESTRA – Recent progress, mode design and signal processing
In *Proc. IEEE Int. Symp. Phased Array Syst. Technol.*, 2019, pp. 1–8.